ACS APPLIED MATERIALS & INTERFACES

Research Article

Cite This: ACS Appl. Mater. Interfaces 2017, 9, 38364-38372

www.acsami.org

Modified Mesoporous Silica Nanoparticles with a Dual Synergetic Antibacterial Effect

Marios Michailidis,*[,†] Ioritz Sorzabal-Bellido,[‡] Evanthia A. Adamidou,[§] Yuri Antonio Diaz-Fernandez,[‡] Jenny Aveyard,[∥] Reut Wengier,[#] Dmitry Grigoriev,[⊥] Rasmita Raval,[‡] Yehuda Benayahu,[#] Raechelle A. D'Sa,[∥] and Dmitry Shchukin*[,†]

[†]Stephenson Institute for Renewable Energy, Department of Chemistry, University of Liverpool, Crown Street, Liverpool L69 7ZD, U.K.

[‡]Open Innovation Hub for Antimicrobial Surfaces at the Surface Science Research Centre, University of Liverpool, Oxford Street, L69 3BX Liverpool, U.K.

[§]Manchester Institute of Biotechnology, School of Chemical Engineering and Analytical Science, The University of Manchester, 131 Princess Street, M1 7DN Manchester, U.K.

[∥]Department of Mechanical, Materials and Aerospace Engineering, University of Liverpool, Liverpool L69 3GH, U.K.

[⊥]Fraunhofer Institute for Applied Polymer Research IAP Functional Protein Systems/Biotechnology, Geiselbergstrasse 69, 14476 Potsdam-Golm, Germany

[#]School of Zoology, George S. Wise Faculty of Life Sciences, Tel Aviv University, Ramat Aviv, Tel Aviv 69978, Israel

Supporting Information

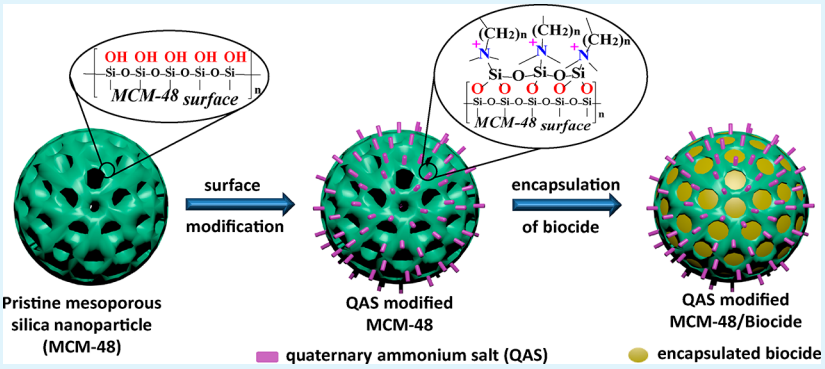

ABSTRACT: Application of mesoporous silica nanoparticles (MSNs) as antifouling/antibacterial carriers is limited and specifically with a dual synergetic effect. In the present work, MSNs modified with quaternary ammonium salts (QASs) and loaded with the biocide Parmetol S15 were synthesized as functional fillers for antifouling/antibacterial coatings. From the family of the MSNs, MCM-48 was selected as a carrier because of its cubic pore structure, high surface area, and high specific pore volume. The QASs used for the surface modification of MCM-48 were dimethyloctadecyl[3-(trimethoxysilyl)propyl]ammonium chloride and dimethyltetradecyl[3-(triethoxysilyl)propyl]ammonium chloride. The QAS-modified MCM-48 reveals strong covalent bonds between the QAS and the surface of the nanoparticles. The surface functionalization was confirmed by Fourier transform infrared spectroscopy, thermogravimetric analysis, elemental analysis, and ζ-potential measurements. Additional loading of the QAS-modified MCM-48 with a commercially available biocide (Parmetol S15) resulted in a synergetic dual antibacterial/antifouling effect. Either loaded or unloaded QAS-modified MSNs exhibited high antibacterial performance confirming their dual activity. The QAS-modified MCM-48 loaded with the biocide Parmetol S15 killed all exposed bacteria after 3 h of incubation and presented 100% reduction at the antibacterial tests against Gram-negative and Gram-positive bacteria. Furthermore, the QAS-modified MCM-48 without Parmetol S15 presented 77−89% reduction against the exposed Gram-negative bacteria and 78−94% reduction against the exposed Gram-positive bacteria. In addition, the modified MCM-48 was mixed with coating formulations, and its antifouling performance was assessed in a field test trial in northern Red Sea. All synthesized paints presented significant antifouling properties after 5 months of exposure in real seawater conditions, and the dual antifouling effect of the nanoparticles was confirmed.

KEYWORDS: *colloids, silica, surface modification, porous materials, nanoparticles, quaternary ammonium salts, encapsulation*

INTRODUCTION

The definition of biofouling or biological fouling is the accumulation of microorganisms, plants, algae, or animals on wetted surfaces. From the first minute of immersion of a clean surface in natural seawater, it immediately starts to adsorb a

Received: September 26, 2017
Accepted: October 12, 2017
Published: October 12, 2017

DOI: 10.1021/acsami.7b14642
ACS Appl. Mater. Interfaces 2017, 9, 38364−38372

molecular conditioning film consisted of dissolved organic materials.[1] After that initial stage, the surface colonization by a wide range of organisms depends on their relative rate of attachment and surface exploitation.[1,2] According to the literature, surface colonization follows a linear "successional model" in which biofilm formation starts within a week by spores of macroalgae (seaweeds), fungi, and protozoa, and after that within several weeks by larvae of invertebrates such as barnacles.[3,4] This classical view is a simplification, as motile spores of seaweeds are capable of settling within minutes on a clean surface, and larvae of some species of barnacles or bryozoans settle within a few hours of immersion.[1] The distinction between the different fouling stages comprises "microfouling", "soft macrofouling", and "hard macrofouling". Microfouling usually refers to microorganisms such as protozoa, bacteria, and diatoms, forming complex biofilms during the first 24 h of immersion. Soft macrofouling comprises the formation of microscopically visible algae, seaweeds, and invertebrates such as soft sponges, corals, tunicates, and anemones after 2 or 3 weeks of immersion. Hard macrofouling refers to the colonization of mussels, barnacles, ascidians, and so forth.

Biofouling has serious effects in various sectors of maritime industry. It is the main expense of maintenance for any immersed man-made surface such as buoys, membrane bioreactors and desalination units, power plants' cooling water systems, and oil pipelines. Furthermore, it has significant effects on the aquaculture industry especially in marine finfish aquaculture where the use of sea cages is necessary. In the ship industry, the adhesion of marine algae and barnacles on the hulls of the ships makes them rough and causes increased erosion, reduction of speed, increased fuel consumption (up to 40%) and, consequently, increases air pollution and CO_2 emission.[5,6] As the diversity of fouling organisms is vast and the range of adhesion mechanisms correspondingly broad, it is a major challenge to create an effective fouling-resistant coating.

The majority of the coatings in the past were biocide-based self-polishing coatings, and their main component was the tributyltin (TBT), an efficient and versatile biocide.[7] The main applications of this biocide were for wood preservation, antifungal applications in industrial processes, marine antifoulings, and as pesticides. However, because of their toxicity to humans and their negative impact on the environment, TBT compounds were prohibited worldwide after 1 January, 2003, and their use as ship coating was completely banned after 1 January, 2008, by the International Convention on the Control of Harmful Anti-fouling Systems on Ships of the International Maritime Organization.[8,9] Subsequently, antifouling manufacturers have been forced to urgently develop new and more environmentally friendly antifouling paints. Almost all antifouling paints today contain copper as their primary active ingredient which is well-known for more than 2000 years from ancient years. Since 300 B.C., Greeks and Romans used copper in the bronze-shod rams of their warships and copper nails to secure the lead sheathing.[7,10]

To date, the working principle of the most of paint systems applied is based on slow release of biocide compounds. This operating principle has drawbacks for the paint systems.[11] Usually, the main active ingredient dissolves away, and the paint loses its effectiveness but the binder stays behind.[7] Furthermore, as more coats are applied, the dead binder layers get thicker and thicker until they start to flake off in large chunks. Thus, it is very difficult and expensive to remove the old paint, and as a consequence, this type of coatings has been put aside. In addition, the antifouling release materials such as perfluorinated or silane-containing compounds were directly introduced into the coating, thereby influencing other coating properties such as corrosion protection. One approach to eliminate some of these drawbacks is encapsulation, a methodology that has been applied into effective delivery systems for various applications in biotechnology, energy storage systems, protection against corrosion, pharmaceutics, and food industry.[12−14] Commonly used technologies to encapsulate small molecules such as biocides include the layer-by-layer method and physical adsorption into porous materials.[15−17] By using proper carriers for encapsulation, it is possible to decrease and control the release rate of biocides and provide an effective protection from the surrounding environment.[18,19]

The quaternary ammonium salts (QASs) have been indexed as antimicrobial compounds for more than 70 years.[20,21] They have been used against the growth of a broad range of microorganisms in several applications including food and pharmaceutical products, antiseptics, disinfectants, biocides, fungicides, cosmetics, and water treatment.[22,23] The QASs are positively charged cationic compounds, and the bacterial cell membranes are negatively charged. As a consequence of electrostatic interactions, the QASs can be adsorbed on the cell surfaces and diffuse through the cell wall. The next step is their binding to the cytoplasmic membrane, causing its disruption and release of K^+ ions and constituents of the cytoplasmic membrane which leads to cell death.[24,25] The effectiveness of the QASs in killing a wide range of microorganisms as antimicrobial agents attracted the interest of scientists. In several studies, QASs were used to functionalize surfaces of different materials as antimicrobial treatment.[24−28] The advantage of the QAS-modified materials in comparison with the classic biocide-release coatings can be attributed to their attachable nature to the fillers of the coatings which allows a permanent antifouling effect of the coating without the release of the biocide material. There are several parameters which influence the interactions between the quaternary ammonium moieties and the cell membranes and therefore their biocidal activity. The effectiveness of a specific QAS is dependent on microorganisms because there are variations to the composition and structure from one microorganism to another.[29] An important parameter for the efficiency of the QAS is the alkyl chain length of their general molecular formula (NR_4^+). It has been found that the QAS with an alkyl chain length of C8 and higher presents high antimicrobial activity.[30]

This work is focused on the development of functional fillers for antibacterial/antifouling coatings with advanced performance compared to the current state of the art coatings. Usually in the literature describing biomedical and antifouling systems, nonporous silica nanoparticles (NPs) are used only for surface modifications and mesoporous silica NPs (MSNs) only for encapsulation. However, to the best of our knowledge, this is the first study that describes the development of dual-function antibacterial/antifouling MSNs based on the combination of two strategies (surface modification and encapsulation) in one system. Through our approach, we aim to demonstrate for first time the idea of an easy, simple, and straightforward method for the development of dual-functional NPs with a long-lasting effect by using established and effective antibacterial/antifouling compounds. For this purpose, spherical MCM-48 MSNs with a dual synergetic antimicrobial effect were synthesized and tested against Gram-positive and Gram-negative bacteria. For the preparation of MSNs, the modified Stöber's method was used

DOI: 10.1021/acsami.7b14642
ACS Appl. Mater. Interfaces 2017, 9, 38364−38372

according to Schumacher et al. because it is an easy and fast way to obtain MCM-48 at room temperature.[31,32] MCM-48 spherical NPs were chosen for two main reasons. First, their interwoven, branched 3D mesostructure makes them excellent candidates for the loading and release of biocides. Second, this is the first study that reports on the surface modification of MCM-48 with QASs.

The surface of the NPs was modified with two different QASs, dimethyloctadecyl[3-(trimethoxysilyl)propyl]ammonium chloride and dimethyltetradecyl[3-(triethoxysilyl)propyl]ammonium chloride. This modification provides the coatings the necessary hydrophobicity and antifouling properties, biocidal activity against marine microorganisms, and resistance to microfouling in seawater immersion. Afterward, the QAS-modified MSNs were loaded with a liquid biocide (Parmetol S15) for a dual antifouling effect. The active ingredient for the Parmetol S15 is 4,5-dichloro-2-octyl-4-isothiazolin-3-one (DCOIT), a highly hydrophobic compound with good biodegradability and low water solubility. DCOIT received the first Environmental Protection Agency (EPA) Green Chemistry award in 1996 for replacing the TBT in antifouling products and has been successfully used in encapsulation techniques for microcapsules with antifouling properties.[33] The final synthesized materials with the encapsulated biocide exhibit superior performance in the antibacterial tests because of the dual antimicrobial effect from the modified surface with the QAS and from the encapsulated biocide in the mesostructure of the NPs. Through our approach, we aim to prevent the early stages of the biofilm and biofouling formation where everything starts with the attachment of microorganisms on surfaces. Modified NPs with high antibacterial performance are great potential fillers for biofilm and fouling-resistant coatings. The modified MSNs can provide permanent antibacterial properties to the coating formulations even after the release of the biocide because of the existence of the chemically attached QAS groups on the NP surface. A five-month field test trial was also conducted to examine the antifouling performance of the synthesized and modified NPs after their addition into coating formulations. PVC panels were coated with the synthesized paints, and after five months of exposure in real seawater conditions, the biofouling coverage was significantly lower compared to the panels coated with the biocide-free Pristine Paint.

RESULTS AND DISCUSSION

Synthesis and Characterization of MCM-48. MCM-48 spherical MSNs were chosen as carriers for the antifouling/antibacterial compounds. MCM-48 can be easily functionalized, as they exhibit high surface reactivity because of the existence of the hydroxyl groups on their surface. In addition, their interwoven, branched 3D mesoporous structure makes them excellent candidates for the loading and release of biocides. For the synthesis of the MSNs, the modified Stöber's method was used as reported by Schumacher et al.[31,32] The powder X-ray diffraction (XRD) spectrum of the synthesized MCM-48 after calcination is similar to that given in the literature data (Figure 1).[31] The samples exhibit five Bragg diffraction peaks in the range of $2\theta = 1.5°-10°$ which correspond to the planes (211), (220), (421), (332), and (431). The diffraction peaks can be assigned to the typical cubic space group *Ia*3*d* characteristic of mesoporous materials with a 3D cubic structure. The planes (211) and (220) are intense and sharp which is an indication of high ordering of our synthesized MCM-48.

The low-temperature nitrogen isotherms can provide accurate and reliable information associated with the specific surface area and the quality of the mesoporous structure of solid materials.[34] The sample presented type IV isotherm according to the Brunauer−Deming−Deming−Teller classification which is characteristic of MCM-41 and MCM-48 mesoporous materials.[35] From the adsorption and desorption isotherm, no hysteresis was observed, and they showed a sharp capillary condensation step which provides information for uniform pore channels and narrow pore size distribution (Figure S1a).[36−39]

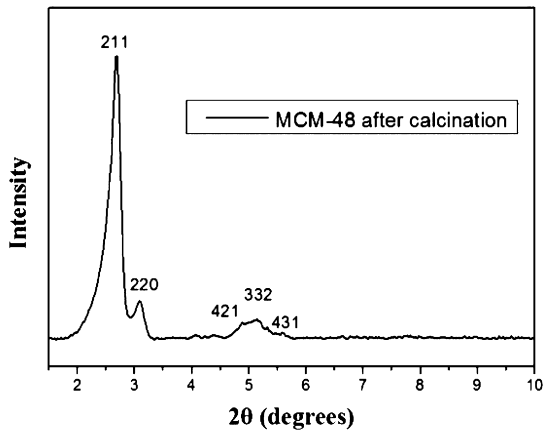

Figure 1. XRD patterns for the synthesized MCM-48 mesoporous NPs; planes (211), (220), (421), (332), and (431) correspond to the cubic space group *Ia*3*d*.

The specific surface area was calculated according to the Brunauer−Emmett−Teller (BET) method, and the mesoporous MCM-48 samples exhibited high values of S_{BET} in a range from 1180 to 1300 m^2/g.[40] The pore size distribution and the total pore volume of the synthesized MCM-48 materials were calculated from the nitrogen adsorption isotherms by using the nonlocal density functional theory (NLDFT) method.[41−43] It has been well-documented that the NLDFT model is a more accurate and rigorous approach for the interpretation of the nitrogen isotherms and the calculation of mesoporous structure properties for MCM-48 materials.[31,32,44,45] The synthesized MCM-48 material presented a high total pore volume of 0.8 cm^3/g at 0.99 relative pressure. Furthermore, the material under study exhibited narrow pore size distribution as expected because of the sharp capillary condensation step (Figure S1b). The average pore diameter is 3.2 nm as calculated from the NLDFT method.

Scanning electron microscopy (SEM) was used to observe the morphology of the samples. The SEM images of the mesoporous MCM-48 after calcination at 550 °C are shown in Figure 2. The samples showed spherical morphology in the range of 150−600 nm. In the reaction mixture, the presence of ammonia works as a morphological catalyst responsible for the spherical size of the particles.[46] As can been seen from the SEM images, some of the particles are aggregated and fused together, but most of them are single monodispersed particles.

Surface Modification with QAS. MCM-48s modified with QASs were characterized by thermogravimetric analysis (TGA), Fourier transform infrared (FTIR) analysis, elemental analysis, and ζ-potential measurements. The FTIR spectra for the pristine MCM-48, QC14-, and QC18-modified MCM-48, are shown in Figure 3. All samples present the characteristic absorption peaks for the SiO_2 materials: Si−O−Si bending vibration (465 cm^{-1}), Si−O−Si symmetric stretching (800 cm^{-1}), Si−OH asymmetric vibration (940 cm^{-1}), Si−O asymmetric vibration (1080 cm^{-1}), H−O−H bending vibration (1635 cm^{-1}), and −OH stretching

DOI: 10.1021/acsami.7b14642
ACS Appl. Mater. Interfaces 2017, 9, 38364−38372

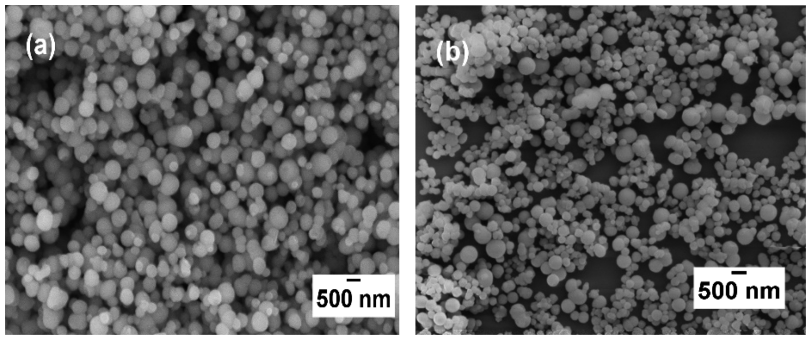

Figure 2. SEM images for the synthesized (a) pristine MCM-48 and (b) QAS-modified MCM-48.

(3400 cm^{-1}). However, the QAS-modified samples showed three additional peaks. These peaks represent the alkyl chain of the QASs and prove that the silica NP was successfully decorated by the QAS. The peak at 1465 cm^{-1} corresponds to the C−H bending vibration, and the peaks at 2850 and 2950 cm^{-1} correspond to the C−H stretching. Furthermore, the broad −OH peak at 3400 cm^{-1} for the pristine MCM-48 is more intense compared to the QAS-modified MCM-48 because of the free −OH groups on the surface and within the pore channel system of pristine MCM-48. There is also a significant reduction in the intensity of the O−H peak in the QAS-modified MCM-48 spectra (Supporting Information, Figure S2). Therefore, the H−

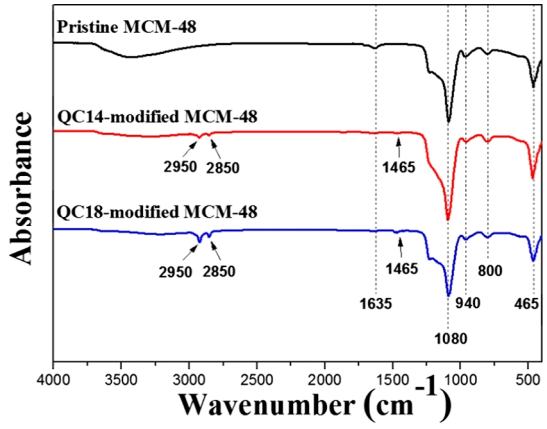

Figure 3. FTIR spectra for pristine MCM-48, QC14-, and QC18-modified MCM-48.

O−H bending vibration (1635 cm^{-1}) and −OH stretching (3400 cm^{-1}) for the QAS-modified MCM-48 will give a very low signal, as most of the available hydroxyl groups reacted with the QAS.

Further information about the surface properties of the modified and unmodified materials was obtained via ζ-potential measurements and elemental analysis (Table 1). The surface of the pristine MSN is positively charged at pH below its isoelectric point (IEP = pH 2.0) and negatively charged above the IEP.[47] At the pH range from 1.5 to 9.5, the ζ-potential for the QAS-modified NPs was shifted significantly to positive values because of the presence of the positively charged quaternary ammonium groups on the surface of the materials instead of the negatively charged hydroxyl groups. Taking into consideration the high values of ζ-potential for the QAS-modified materials (between +40 and +60 mV), we can hypothesize that the modified particles have good stability in colloidal suspensions. Further confirmation of the successful surface modification comes from the elemental analysis. The QC18- and QC14-modified particles showed significant increment of % C, % H, and % N compared to the pristine MCM-48 because of the alkyl functional groups and the positively charged nitrogen groups of the covalently attached QAS moieties (Table 1).

The TGA was used to evaluate the amount of the QAS grafted on the surface of the MSNs when heated under N_2 atmosphere up to 800 °C (Figure 4). The pristine MCM-48 was calcinated up to 800 °C, and its weight decreased only by 4% mainly because of the decomposition of silanol groups and the existence of some humidity inside the material. The silica NPs have very high thermal stability and almost keep their weight constant up to 800 °C at least. However, when QC18- or QC14-modified MCM-48s NPs were calcinated to 800 °C, they lost 28.3 and 19.2% of their initial weight, respectively. Both QC18- and QC14-modified MCM-48 presented 3% weight loss between 30 and 130 °C because of humidity and decomposition of unreacted silanol groups. The further 25.3 or 16.2% weight loss between 200 and 800 °C is attributed to the calcination of the attached QC18 or QC14 groups, respectively.

Significant differences between the two types of modified materials at the TGA and the ζ-potential measurements and the elemental analysis are caused by two main reasons. First, there are four extra $-CH_2$ groups in the alkyl chain of the QC18 molecule compared to the QC14 molecule. Therefore, we expected higher weight loss and higher % of C and H for the QC18-modified material at the TGA measurements and elemental analysis. Second, the QC18 compound was commercially available at 99% purity, whereas the QC14

Table 1. ζ-Potential Measurements (Right) and Elemental Analysis (Left) for the Pristine, QC18-, and QC14-Modified MCM-48

Sample	Elemental analysis (wt%)		
	C	H	N
Pristine MCM-48	1.08	0.53	0
QC18-modified MCM-48	20.24	3.95	0.98
QC14-modified MCM-48	15.12	3.09	0.73

pH value	Pristine MCM-48 (mV)	QC18-modified MCM-48 (mV)	QC14-modified MCM-48 (mV)
1.5	3.0 ±1	32.5 ±2	30.1 ±1
4	-31.0 ±2	63.3 ±2	49.2 ±1
7.5	-28.3 ±1	52.8 ±1	43.0 ±2
9.5	-33.9 ±1	50.1 ±1	35.8 ±1

DOI: 10.1021/acsami.7b14642
ACS Appl. Mater. Interfaces 2017, 9, 38364−38372

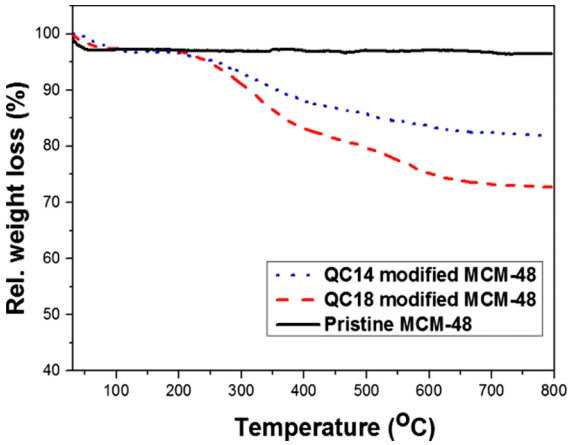

Figure 4. TGA curves for the pristine MCM-48, QC18-modified MCM-48, and QC14-modified MCM-48.

compound is commercially unavailable and as a result was synthesized in-house. The dimethyltetradecyl[3-(triethoxysilyl)-propyl]ammonium chloride (QC14) was synthesized by reacting 1.97×10^{-2} mol of *N*,*N*-dimethyltetradecylamine with 2.08×10^{-2} mol of 3-chloropropyltriethoxy silane at 110 °C for 48 h. After the reaction, the color of the solution became yellow-brown and the viscosity increased confirming the quaternization reaction (Supporting Information, Figures S3 and S4). Proton nuclear magnetic resonance (^{1}H NMR) spectroscopy was used to confirm the successful synthesis of the QC14 (Supporting Information, Figure S5). The ^{1}H NMR spectrum of the product (QC14) showed two additional peaks at 3.38 ppm [$-N^+-(CH_3)_2$] and 3.46 ppm ($-N^+-CH_2$) because of the quaternization. However, the presence of the peaks at 3.54 ppm ($-CH_2-Cl$) and 2.2 ppm [$-N-(CH_3)_2$] after 48 h of reaction indicate that there are residual *N*,*N*-dimethyltetradecylamine and 3-chloropropyltriethoxy silane. Thus, during the surface modification of the MCM-48 with QC14, the available silanol groups on the MCM-48 surface can react both with the 3-chloropropyltriethoxy silane and the QC14. As a result, the surface of the QC14-modified MCM-48 is covered with QC14 molecules and 3-chloropropyltriethoxy silane molecules. Our hypothesis is confirmed by the decreased amount of nitrogen in elemental analysis, the decreased positive values of ζ-potential measurements and the lower weight loss on the TGA curve for the QC14-functionalized silica compared to the QC18-functionalized silica.

Encapsulation of Biocide. Encapsulation is an important technology that finds applications in pharmaceutical industry, food industry, energy storage systems, etc., by using materials such as MSNs, polymeric capsules, hydrogels, and so forth as hosts.[48,49] In our approach for the encapsulation of the Parmetol S15 biocide, the two different types of modified MCM-48s were dispersed directly via sonication in the commercially available liquid biocide Parmetol S15 and left under vacuum overnight. After the recovery of the solid materials with the encapsulated biocide, the samples were tested with the TGA, and the amount of the loaded biocide was measured. The TGA curves of the QAS-modified MCM-48 loaded with the Parmetol S15 were compared with the TGA curves of the unloaded QAS-modified MCM-48 (Figure 5). The loaded QC18-modified MCM-48 with Parmetol showed 26.9 wt % additional weight loss in comparison with the unloaded QC18-modified MCM-48 because of the encapsulated biocide. The loaded QC14-modified MCM-48 with Parmetol exhibited 31.5 wt % further weight loss in comparison with the unloaded QC14-modified MCM-48, which is also attributed to the encapsulated biocide. The TGA curves confirmed the successful encapsulation of the biocide inside the MSNs. During the surface modification, the $-Si(OCH_3)_3$ groups of the quaternary silane are covalently bonded with $-OH$ groups close to the opening of the pores, thus blocking some of the pores for the biocide ingress. Moreover, in the case of the QC18-modified MSNs, the blockage of the pores is higher because of its larger molecular size. This can explain the 4.6 wt % lower amount of the encapsulated biocide inside the QC18-modified MCM-48 compared to the amount encapsulated inside the QC14-modified MCM-48.

Antibacterial Performance. For the evaluation of the antibacterial activity of synthesized materials, 22 mm × 22 mm glass slides were coated with a spin coater by using 1 mL of these particles dispersed in ethanol solution (2 wt %) and tested against Gram-negative *Escherichia coli* and Gram-positive *Staphylococcus aureus*. The pristine MCM-48 was used as a negative control because no antibacterial activity is expected from this material. The relative number of viable bacteria adhered on the glass slide coated with pristine MCM-48 was defined as 100%. As can been seen from Figure 6, the QC18- and QC14-modified MSNs reduced the number of the viable bacteria *E. coli* by 89 and 77%, respectively, compared to the pristine MCM-48,

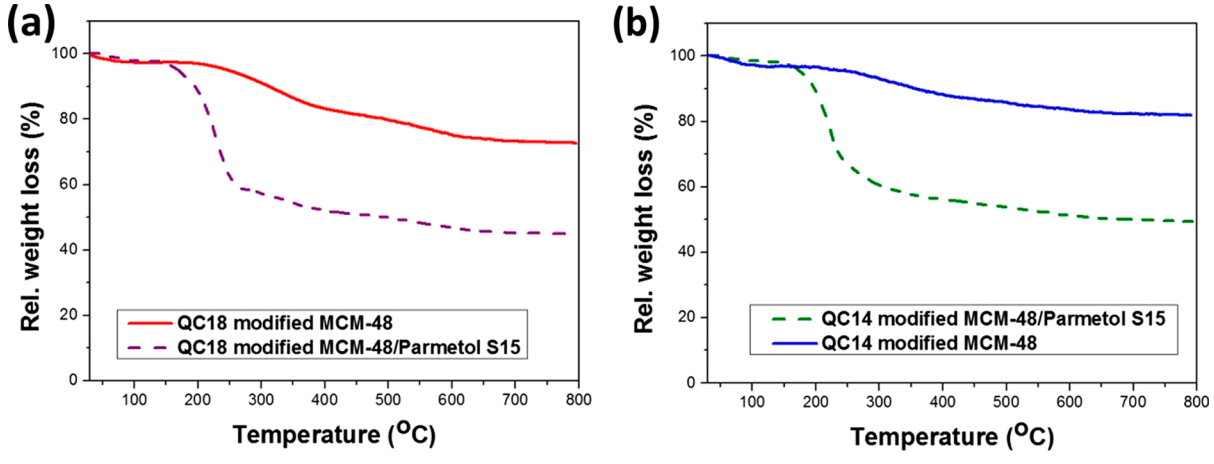

Figure 5. TGA curves for (a) the loaded/unloaded QC18-modified MCM-48 and (b) the loaded/unloaded QC14-modified MCM-48.

DOI: 10.1021/acsami.7b14642
ACS Appl. Mater. Interfaces 2017, 9, 38364−38372

whereas the two types of modified MSNs with the encapsulated Parmetol S15 presented excellent and enhanced antibacterial performance by killing all exposed bacteria during the test, resulting in 100% reduction compared to the pristine MCM-48.

Figure 7 shows the antibacterial performance of the pristine and modified MCM-48 against the Gram-positive bacteria *S. aureus*. The QC18-and QC14-modified MCM-48 reduced the relative number of viable bacteria by 94 and 78%, respectively. The QC18- and QC14-modified MCM-48 loaded with the additional biocide Parmetol S15 exhibited 100% reduction by killing all exposed bacteria at the end of the experiment. In the antibacterial tests against both types of bacteria, there is a statistically significant ($p < 0.0005$) increase in the antibacterial

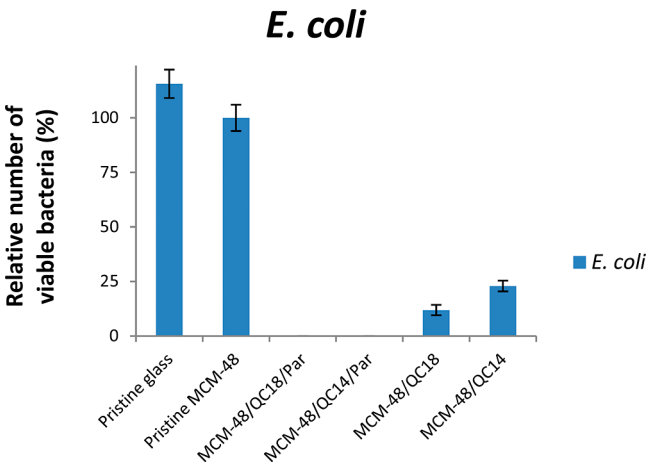

Figure 6. Relative number of viable bacteria (*E. coli*) after testing on glass slides spin-coated with pristine MCM-48, loaded/unloaded QC18- and QC14-modified MCM-48. Statistically significant differences between the samples ($p < 0.0005$).

activity when the pristine MCM-48s are either modified only with QAS or modified with QAS and loaded with Parmetol S15.

It is noteworthy that the QC18-modified MSNs presented higher antibacterial performance against *E. coli* and *S. aureus* in comparison with the QC14-modified MSNs. As mentioned previously, the surface of the QC14-modified MCM-48 is covered with QC14 molecules and 3-chloropropyltriethoxy silane molecules because after the quaternization reaction of the QC14, there was residual 3-chloropropyltriethoxy silane. Therefore, the QC18-modified MCM-48s have a higher amount of quaternary ammonium groups than the QC14-modified MCM-48, which is confirmed by the elemental analysis (Table 1). There are several studies supporting the fact that increased numbers of quaternary ammonium groups result in increasing the antibacterial performance of the compound.[50,51] In addition, according to the killing mechanism of the QAS, the longer the alkyl chain length of the quaternary compound, the easier it penetrates the cell membrane and causes the death of the bacteria. As a consequence, the QC18-modified MCM-48 exhibited increased antibacterial performance compared to the QC14-modified MCM-48. The results from the antibacterial tests against *S. aureus* and *E. coli* come as a confirmation of the dual synergetic antibacterial effect of the QAS-modified MSNs with the encapsulated Parmetol S15. The antibacterial effect will be permanent even after the release of the encapsulated biocide because of the presence of the covalently attached QAS on the NP surface.

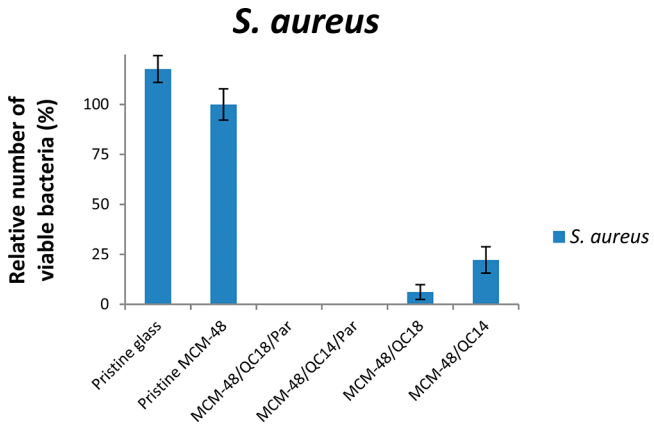

Figure 7. Relative number of viable bacteria (*S. aureus*) after testing on glass slides spin-coated with pristine MCM-48, loaded/unloaded QC18- and QC14-modified MCM-48. Statistically significant differences between the samples ($p < 0.0005$).

Antifouling Performance of Coated PVC Panels with the Synthesized Paints. A panel field test took place in northern Red Sea, Eilat, Israel, for a five-month period to evaluate the antifouling efficacy of the modified MCM-48 NPs incorporated in coatings. PVC panels coated with Pristine Paint (biocide-free paint) were used as control samples. QC18-modified MCM-48 loaded with Parmetol S15, QC14-modified MCM-48 loaded with Parmetol S15, QC18-modified MCM-48, and QC14-modified MCM-48 were added in 5 wt % concentration into the Pristine Paint, and the paints 1−4 were synthesized. Figure 8 illustrates photographs of the exposed coated panels in the first day of deployment after five months of exposure. At the end of the field test, the control sample coated with the Pristine Paint presented 39% biofouling coverage, whereas the paints 1−4 presented significantly lower biofouling coverage below 10%. In particular, paints 1 and 2 containing the modified NPs with the dual effect illustrated superior performance with 6.7 and 7.8% biofouling coverage because of the encapsulated biocide into the QAS-modified NPs, confirming their enhanced antifouling effect. Furthermore, paints 3 and 4 containing the QAS-modified NPs exhibited 8.4 and 9.8% biofouling coverage, respectively, suggesting that even after the release of the encapsulated biocide, the QAS groups on the surface of the NPs will continue to provide antifouling properties to the coating formulations.

CONCLUSIONS

The MCM-48 MSNs with an average size of 400 nm were successfully synthesized as shown by the XRD, SEM, and BET measurements. The synthesized materials presented XRD patterns characteristic of highly ordered 3D mesoporous structures. In the second step, the MSN surface modified with QASs {either dimethyloctadecyl[3-(trimethoxysilyl)propyl]-ammonium chloride (QC18) or dimethyltetradecyl[3-(triethoxysilyl)propyl]ammonium chloride (QC14)} was successfully synthesized, revealing strong covalent bonds between the QASs and the surface of the NPs. The surface functionalization was confirmed by FTIR, TGA, elemental analysis, and ζ-potential measurements. The FTIR spectra for the modified materials showed three additional peaks, confirming the presence of C−H bonds due to the attached QASs on the MCM-48 surface. The TGA curves showed 19−28 wt % further weight loss for the modified MSNs because of the

DOI: 10.1021/acsami.7b14642
ACS Appl. Mater. Interfaces 2017, 9, 38364−38372

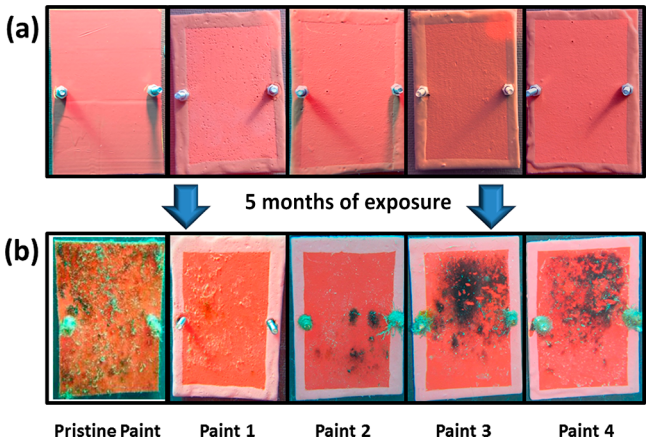

Figure 8. Photographs of PVC panels coated with Pristine Paint and paints 1−4 for the field test trial (Eilat, northern Red Sea) in the first day of deployment (a) and after 5 months of exposure (b).

QAS calcination. The ζ-potential presented significant change of the surface charges from negative to positive (>80 mV) after the modification of the negatively charged silica with positively charged quaternary ammonium groups. To achieve the dual synergetic effect, the synthesized materials were loaded with one additional biocide for an enhanced dual antibacterial/antifouling effect.

The encapsulation of the biocide Parmetol S15 was confirmed by the TGA curves where the loaded materials presented 31.5 wt % (QC18-modified) and 26.9 wt % (QC14-modified) of weight loss compared to the unloaded materials. In the antibacterial tests, all synthesized modified NPs exhibited high antibacterial performance, confirming their dual activity. In the case of the QAS-modified MCM-48 loaded with the biocide Parmetol S15, all exposed bacteria were dead at the end of the experiments for both antibacterial tests against Gram-negative and Gram-positive bacteria. Furthermore, the QAS-modified MCM-48 presented 77−89% reduction against Gram-negative bacteria and 78−94% reduction against Gram-positive bacteria. Finally, the modified NPs were incorporated into coating formulations, and their antifouling activity was assessed in a field test trial. All synthesized paints illustrated significant antifouling activity, and the biofouling coverage was considerably lower compared to the biocide-free Pristine Paint. The results from the field test provide a confirmation of the dual antifouling activity of the synthesized NPs that can be used as potential functional fillers for tin-free alternative paints in marine industry.

Through our approach, we propose for the first time a quick and effective way to synthesize antibacterial NPs with a dual synergetic effect and excellent and permanent performance. In our studies, we used a commercially available biocide for the encapsulation. However, because of the hydrophobic nature of the QAS-modified MSNs, other biocides or antibacterial agents can be used for the encapsulation. The modified particles with the dual synergetic effect can be excellent carriers of antibacterial/antifouling compounds for coating formulations in several applications such as hospitals, marine industry, and so forth.

MATERIALS AND METHODS

Materials. For the synthesis of the MSNs, tetraethyl orthosilicate (TEOS 98%, Sigma-Aldrich) was used as the source of silica and hexadecyltrimethylammonium bromide (CTAB 99%, Sigma-Aldrich) was used as a surfactant (structure directing agent). Ethanol (99.8%, Sigma-Aldrich) and ammonium hydroxide (32%, Merck) were used to carry out the synthesis of MSNs. Dimethyloctadecyl[3-(trimethoxysilyl)propyl]ammonium chloride (QC18 60% in methanol, Acros Organics) and dimethyltetradecyl[3-(triethoxysilyl)propyl]-ammonium chloride (QC14) were the QASs used for the surface modification of the MSNs. The biocide for loading the MSNs was Parmetol S15 (Schulke). The chemical composition of Parmetol is similar to SeaNine, as in both biocides, the active compound is DCOIT. Parmetol S15 can be easily encapsulated into the mesostructure of our MSNs because of its better compatibility with the hydrophobic pore channel system of the QAS-modified MSNs.

Synthesis of MSNs with an Average Size of 400 nm. The modified Stöber's method was used for the synthesis of MSNs as reported by Schumacher et al.[31,32] According to this method, spherical MCM-48s can be synthesized at room temperature. In a typical synthesis route, CTAB (2.6 g, 6.6 mmol) was dissolved in a mixture of deionized water (120 mL) and pure ethanol (50 mL, 0.87 mol), and ammonium hydroxide (12 mL of 32 wt % solution) was added to the surfactant solution. The solution was stirred for 10 min at 600 rpm, and TEOS (3.4 g, 16 mmol) was added at once during stirring. After stirring for 16 h at room temperature, the resulting solid was recovered by filtration, washed twice with ethanol, twice with distilled water, and dried in air under ambient conditions. The organic template was removed by calcination in a muffle furnace at 550 °C for 6 h after heating with a ramp of 1 °C/min.

Synthesis of Dimethyltetradecyl[3-(trimethoxysilyl)propyl]-ammonium Chloride (QC14). The dimethyltetradecyl[3-(triethoxysilyl)propyl]ammonium chloride (QC14) was synthesized by reacting 4.76 g of *N*,*N*-dimethyltetradecylamine (1.97×10^{-2} mol) with 5 g of 3-chloropropyltriethoxy silane (2.08×10^{-2} mol) in a 20 mL vial. The vial containing the reaction mixture was purged with nitrogen for 10 min before sealing. The quaternization reaction was carried out at 110 °C for 48 h using magnetic stirring. After 48 h, the reaction mixture was cooled at room temperature before adding 9.76 g of methanol to produce 50 wt % solution of dimethyltetradecyl[3-(trimethoxysilyl)-propyl]ammonium chloride (QC14) in methanol.[52]

Surface Modification of the MSNs. The QAS-modified MCM-48 was prepared by hydrolysis and condensation reactions between the QAS and the hydroxyl groups on the surface of the MCM-48 (Supporting Information, Figure S2). For the surface modification, 1 g of calcinated MCM-48 powder was dispersed in a mixture of ethanol (50 mL) and deionized water (50 mL) using sonication bath. To the homogeneous solution, 0.5 mL of either QC18 or QC14 was added and stirred for 24 h at room temperature. The modified NPs were collected with centrifugation, washed twice with ethanol and twice with water to remove the residual reagents, and dried under ambient conditions.

Loading the Modified MSNs with Biocide. Before loading the modified MSNs, the samples were dried at 100 °C under vacuum to remove water and air from the mesoporous structure. Subsequently, modified MSNs (0.20 g) were dispersed directly in the biocide Parmetol S15 (20 mL) and stirred under vacuum overnight. The solid was recovered by filtration and gently washed on the filter paper dropwise with ethanol. The loaded NPs were dried under ambient conditions.

Characterization Methods. The powder XRD patterns were obtained on a Bruker diffractometer using Cu Kα radiation. The morphology of the samples was observed using the scanning electron microscope JEOL 7001F. The TGA curves were obtained at the Linseis STA PT-1000 instrument with calcination temperature up to 800 °C under nitrogen. The chemical structure of the modified NPs was confirmed by recording their FTIR spectra in the wavenumber range from 4000 to 400 cm^{-1} using the Bruker TENSOR II instrument. The ζ-potential for pristine and modified samples (dispersed in aqueous solutions under ambient conditions) was measured using the Malvern Zetasizer Nano ZS instrument. Nitrogen adsorption isotherms were measured at 77 K on a Quadrasorb SI analyzer (Quantachrome Instruments). Before the measurements, the samples were outgassed for 20 h at 423 K. The elemental analysis values were obtained using a Flash EA 1112 organic elemental analyzer.

Antibacterial Activity of Pristine and Modified MCM-48. *S. aureus* (ATCC 25923) and *E. coli* (ATCC 10536) cultures were grown

DOI: 10.1021/acsami.7b14642
ACS Appl. Mater. Interfaces 2017, 9, 38364−38372

overnight at 37 °C in sterilized nutrient broth (NB) medium. The bacterial cells were centrifuged, and the NB was replaced by a sterile 500-fold diluted NB (1/500 NB). For the tests against Gram-negative *E. coli* and Gram-positive *S. aureus*, 22 mm × 22 mm glass slides were coated by 1 mL of either pristine or modified NPs dispersed in ethanol solution (2 wt %) with a spin coater. The samples used for the antibacterial tests were as follows: pristine glass, pristine MCM-48, QC18-modified MCM-48 loaded with Parmetol S15, QC14-modified MCM-48 loaded with Parmetol S15, QC18-modified MCM-48 and QC14-modified MCM-48. The pristine MCM-48 was used as a negative control because no antibacterial activity is expected from this material. The spin-coated glass slides were UV-sterilized for 1 h and were inoculated with 50 μL of 10^5 colony forming unit per mL (cfu/mL) of either *S. aureus* or *E. coli* solution. Each sample was covered with a 20 mm × 20 mm sterile glass cover slip and was incubated at 37 °C for 3 h. Then, each sample was introduced in a 50 mL falcon tube containing 10 mL of phosphate-buffered saline solution and was vortexed prior to spreading 100 μL of the bacterial solution on an agar plate. Inoculated agar plates were incubated overnight, and the cfu/mL was counted. Each sample type was studied in triplicate following this method. One-way analysis of variance was used to compare mean values to determine the equivalence of variance between the samples. Significance between the samples was determined using the Bonferroni multiple comparison test where a value of $p < 0.05$ was taken as statistically significant.

Antifouling Activity of Coating Formulations Containing Modified MCM-48 (Field Test). For the preparation of the test paints, as-synthesized modified MCM-48s were suspended mechanically via a homogenizer in a polymeric paint matrix. The polymeric paint matrix (Pristine Paint) was developed specifically for the EU FP7 BYEFOULING project by Jotun, and it is a solvent-based biocide-free coating formulation. The concentration of the NPs in the paints was adjusted to 5 wt %, and four different paint formulations were synthesized. Paint 1: Pristine Paint +5 wt % QC18-modified MCM-48 loaded with Parmetol S15, paint 2: Pristine Paint +5 wt % QC14-modified MCM-48 loaded with Parmetol S15, paint 3: Pristine Paint +5 wt % QC18-modified MCM-48, and paint 4: Pristine Paint +5 wt% QC14-modified MCM-48.

PVC panels of 7 × 10 cm coated with five different types of paints (Pristine Paint and paints 1−4) were immersed in the Red Sea, Eilat, Israel, for a five-month field test trial for a realistic assessment of their antifouling properties. The coated PVC panels were placed on a floating structure made of a stainless steel frame on which two PVC boards were attached and submerged at a depth of 8−9 m (Figure S7). Each panel was attached by nuts to two stainless steel bolts. The panels were photographed underwater during the exposure period, and the percentage of fouling covering the panels was determined by using the image analysis software Image J.[53] The quantification of the fouling and the biofilm provided a round overview of the coating performance.

■ ASSOCIATED CONTENT

Supporting Information

The Supporting Information is available free of charge on the ACS Publications website at DOI: 10.1021/acsami.7b14642.

Further information about the mechanism of surface modification, reaction of synthesis for the QC14, and ^{1}H NMR spectra and images for the synthesized materials (PDF)

■ AUTHOR INFORMATION

Corresponding Authors

*E-mail: Marios.Michailidis@liverpool.ac.uk (M.M.).
*E-mail: D.Shchukin@liverpool.ac.uk (D.S.).

ORCID

Marios Michailidis: 0000-0001-8845-2375
Dmitry Grigoriev: 0000-0001-6961-1000
Dmitry Shchukin: 0000-0002-2936-804X

Notes

The authors declare no competing financial interest.

■ ACKNOWLEDGMENTS

This work was financially supported by the EU FP7 BYEFOULING project of EU Commission. We thank the Interuniversity Institute for Marine Sciences in Eilat (IUI) for assistance and use of facilities. We acknowledge M. Weis and E. Gunter-Hoch for their help in the field work. This research was in part supported by the Israel Cohen Chair in Environmental Zoology to Y.B. The field test complied with a permit issued by the Israel Nature and National Parks Protection Authority.

■ REFERENCES

(1) Callow, J. A.; Callow, M. E. Trends in the Development of Environmentally Friendly Fouling-Resistant Marine Coatings. *Nat. Commun.* **2011**, *2*, 244.
(2) Callow, M. E.; Callow, J. A. Marine Biofouling: A Sticky Problem. *Biologist* **2002**, *49*, 10−14.
(3) Chambers, L. D.; Stokes, K. R.; Walsh, F. C.; Wood, R. J. K. Modern Approaches to Marine Antifouling Coatings. *Surf. Coat. Technol.* **2006**, *201*, 3642−3652.
(4) Magin, C. M.; Cooper, S. P.; Brennan, A. B. Non-Toxic Antifouling Strategies. *Mater. Today* **2010**, *13*, 36−44.
(5) Schultz, M. P.; Bendick, J. A.; Holm, E. R.; Hertel, W. M. Economic Impact of Biofouling on a Naval Surface Ship. *Biofouling* **2011**, *27*, 87−98.
(6) Fitridge, I.; Dempster, T.; Guenther, J.; de Nys, R. The Impact and Control of Biofouling in Marine Aquaculture: A Review. *Biofouling* **2012**, *28*, 649−669.
(7) Yebra, D. M.; Kiil, S.; Dam-Johansen, K. Antifouling Technology—Past, Present and Future Steps towards Efficient and Environmentally Friendly Antifouling Coatings. *Prog. Org. Coat.* **2004**, *50*, 75−104.
(8) Almeida, E.; Diamantino, T. C.; de Sousa, O. Marine Paints: The Particular Case of Antifouling Paints. *Prog. Org. Coat.* **2007**, *59*, 2−20.
(9) IMO. Focus on IMO: Anti-Fouling Systems. *Int. Marit. Organ.* **2002**, *44*, 1−31.
(10) Adams, J. R.; Antoniadou, A.; Hunt, C. O.; Bennett, P.; Croudace, I. W.; Taylor, R. N.; Pearce, R. B.; Earl, G. P.; Flemming, N. C.; Moggeridge, J.; Whiteside, T.; Oliver, K.; Parker, A. J. The Belgammel Ram, a Hellenistic-Roman Bronze Proembolion Found off the Coast of Libya: Test Analysis of Function, Date and Metallurgy, with a Digital Reference Archive. *Int. J. Naut. Archaeol.* **2013**, *42*, 60−75.
(11) Lejars, M.; Margaillan, A.; Bressy, C. Fouling Release Coatings: A Nontoxic Alternative to Biocidal Antifouling Coatings. *Chem. Rev.* **2012**, *112*, 4347−4390.
(12) Gao, H.; Wen, D.; Sukhorukov, G. B. Composite Silica Nanoparticle/polyelectrolyte Microcapsules with Reduced Permeability and Enhanced Ultrasound Sensitivity. *J. Mater. Chem. B* **2015**, *3*, 1888−1897.
(13) Zheng, Z.; Chang, Z.; Xu, G.-K.; McBride, F.; Ho, A.; Zhuola, Z.; Michailidis, M.; Li, W.; Raval, R.; Akhtar, R.; Shchukin, D. Micro-encapsulated Phase Change Materials in Solar-Thermal Conversion Systems: Understanding Geometry-Dependent Heating Efficiency and System Reliability. *ACS Nano* **2017**, *11*, 721−729.
(14) Zheng, Z.; Schenderlein, M.; Huang, X.; Brownbill, N. J.; Blanc, F.; Shchukin, D. Influence of Functionalization of Nanocontainers on Self-Healing Anticorrosive Coatings. *ACS Appl. Mater. Interfaces* **2015**, *7*, 22756−22766.
(15) Gao, H.; Goriacheva, O. A.; Tarakina, N. V.; Sukhorukov, G. B. Intracellularly Biodegradable Polyelectrolyte/Silica Composite Microcapsules as Carriers for Small Molecules. *ACS Appl. Mater. Interfaces* **2016**, *8*, 9651−9661.
(16) Shchukina, E. M.; Shchukin, D. G. LbL Coated Microcapsules for Delivering Lipid-Based Drugs. *Adv. Drug Delivery Rev.* **2011**, *63*, 837−846.

DOI: 10.1021/acsami.7b14642
ACS Appl. Mater. Interfaces 2017, 9, 38364−38372

(17) Trojer, M. A.; Nordstierna, L.; Bergek, J.; Blanck, H.; Holmberg, K.; Nydén, M. Use of Microcapsules as Controlled Release Devices for Coatings. *Adv. Colloid Interface Sci.* **2015**, *222*, 18−43.
(18) Maia, F.; Silva, A. P.; Fernandes, S.; Cunha, A.; Almeida, A.; Tedim, J.; Zheludkevich, M. L.; Ferreira, M. G. S. Incorporation of Biocides in Nanocapsules for Protective Coatings Used in Maritime Applications. *Chem. Eng. J.* **2015**, *270*, 150−157.
(19) Sørensen, G.; Nielsen, A. L.; Pedersen, M. M.; Poulsen, S.; Nissen, H.; Poulsen, M.; Nygaard, S. D. Controlled Release of Biocide from Silica Microparticles in Wood Paint. *Prog. Org. Coat.* **2010**, *68*, 299−306.
(20) Tischer, M.; Pradel, G.; Ohlsen, K.; Holzgrabe, U. Quaternary Ammonium Salts and Their Antimicrobial Potential: Targets or Nonspecific Interactions? *ChemMedChem* **2012**, *7*, 22−31.
(21) Xue, Y.; Xiao, H.; Zhang, Y. Antimicrobial Polymeric Materials with Quaternary Ammonium and Phosphonium Salts. *Int. J. Mol. Sci.* **2015**, *16*, 3626−3655.
(22) Hegstad, K.; Langsrud, S.; Lunestad, B. T.; Scheie, A. A.; Sunde, M.; Yazdankhah, S. P. Does the Wide Use of Quaternary Ammonium Compounds Enhance the Selection and Spread of Antimicrobial Resistance and Thus Threaten Our Health? *Microb. Drug Resist.* **2010**, *16*, 91−104.
(23) Maillard, J.-Y. Bacterial Target Sites for Biocide Action. *Symp. Ser. Soc. Appl. Microbiol.* **2002**, *31*, 16S−27S.
(24) Tashiro, T. Antibacterial and Bacterium Adsorbing Macromolecules. *Macromol. Mater. Eng.* **2001**, *286*, 63−87.
(25) Davies, A.; Bentley, M.; Field, B. S. Comparison of the Action of Vantocil, Cetrimide and Chlorhexidine on Escherichia Coli and Its Spheroplasts and the Protoplasts of Gram Positive Bacteria. *J. Appl. Bacteriol.* **1968**, *31*, 448−461.
(26) Gottenbos, B.; van der Mei, H. C.; Klatter, F.; Nieuwenhuis, P.; Busscher, H. J. In Vitro and in Vivo Antimicrobial Activity of Covalently Coupled Quaternary Ammonium Silane Coatings on Silicone Rubber. *Biomaterials* **2002**, *23*, 1417−1423.
(27) Nurdin, N.; Helary, G.; Sauvet, G. Biocidal Polymers Active by Contact. II. Biological Evaluation of Polyurethane Coatings with Pendant Quaternary Ammonium Salts. *J. Appl. Polym. Sci.* **1993**, *50*, 663−670.
(28) Saif, M. J.; Anwar, J.; Munawar, M. A. A Novel Application of Quaternary Ammonium Compounds as Antibacterial Hybrid Coating on Glass Surfaces. *Langmuir* **2009**, *25*, 377−379.
(29) Majumdar, P.; He, J.; Lee, E.; Kallam, A.; Gubbins, N.; Stafslien, S. J.; Daniels, J.; Chisholm, B. J. Antimicrobial Activity of Polysiloxane Coatings Containing Quaternary Ammonium-Functionalized Polyhedral Oligomeric Silsesquioxane. *J. Coat. Technol. Res.* **2010**, *7*, 455−467.
(30) Nakagawa, Y.; Hayashi, H.; Tawaratani, T.; Kourai, H.; Horie, T.; Shibasaki, I. Disinfection of Water with Quaternary Ammonium Salts Insolubilized on a PorousGlass Surface. *Appl. Environ. Microbiol.* **1984**, *47*, 513−518.
(31) Schumacher, K.; Grün, M.; Unger, K. K. Novel Synthesis of Spherical MCM-48. *Microporous Mesoporous Mater.* **1999**, *47*, 201−206.
(32) Schumacher, K.; Ravikovitch, P. I.; Du Chesne, A.; Neimark, A. V.; Unger, K. K. Characterization of MCM-48 Materials. *Langmuir* **2000**, *16*, 4648−4654.
(33) Borodina, T. N.; Grigoriev, D. O.; Carillo, M. A.; Hartmann, J.; Moehwald, H.; Shchukin, D. G. Preparation of Multifunctional Polysaccharide Microcontainers for Lipophilic Bioactive Agents. *ACS Appl. Mater. Interfaces* **2014**, *6*, 6570−6578.
(34) Rouquerol, F.; Rouquerol, J.; Llewellyn, P.; Sing, K. S. W.; Maurin, G. *Adsorption by Powders and Porous Solids*; Academic Press, 2013.
(35) Brunauer, S.; Deming, L. S.; Deming, W. E.; Teller, E. On a Theory of the van Der Waals Adsorption of Gases. *J. Am. Chem. Soc.* **1940**, *62*, 1723−1732.
(36) Romero, A. A.; Alba, M. D.; Zhou, W.; Klinowski, J. Synthesis and Characterization of the Mesoporous Silicate Molecular Sieve MCM-48. *J. Phys. Chem. B* **1997**, *101*, 5294−5300.
(37) Kruk, M.; Jaroniec, M.; Ryoo, R.; Joo, S. H. Characterization of MCM-48 Silicas with Tailored Pore Sizes Synthesized via a Highly Efficient Procedure. *Chem. Mater.* **2000**, *12*, 1414−1421.
(38) Kruk, M.; Jaroniec, M.; Ryoo, R.; Kim, J. M. Characterization of High-Quality MCM-48 and SBA-1 Mesoporous Silicas. *Chem. Mater.* **1999**, *11*, 2568−2572.
(39) Vartuli, J. C.; Schmitt, K. D.; Kresge, C. T.; Roth, W. J.; Leonowicz, M. E.; McCullen, S. B.; Hellring, S. D.; Beck, J. S.; Schlenker, J. L. Effect of Surfactant/Silica Molar Ratios on the Formation of Mesoporous Molecular Sieves: Inorganic Mimicry of Surfactant Liquid-Crystal Phases and Mechanistic Implications. *Chem. Mater.* **1994**, *6*, 2317−2326.
(40) Brunauer, S.; Emmett, P. H.; Teller, E. Adsorption of Gases in Multimolecular Layers. *J. Am. Chem. Soc.* **1938**, *60*, 309−319.
(41) Lastoskie, C.; Gubbins, K. E.; Quirke, N. Pore Size Distribution Analysis of Microporous Carbons: A Density Functional Theory Approach. *J. Phys. Chem.* **1993**, *97*, 4786−4796.
(42) Landers, J.; Gor, G. Y.; Neimark, A. V. Density Functional Theory Methods for Characterization of Porous Materials. *Colloids Surf., A* **2013**, *437*, 3−32.
(43) Ravikovitch, P. I.; Domhnaill, S. C. O.; Neimark, A. V.; Schueth, F.; Unger, K. K. Capillary Hysteresis in Nanopores: Theoretical and Experimental Studies of Nitrogen Adsorption on MCM-41. *Langmuir* **1995**, *11*, 4765−4772.
(44) Ravikovitch, P. I.; Haller, G. L.; Neimark, A. V. Adsorption Characterization of Mesoporous Molecular Sieves. *Mesoporous Molecular Sieves 1998, Proceedings of the 1st International Symposium*, 1998; Vol. *117*, pp 77−84.
(45) Neimark, A. V.; Ravikovitch, P. I.; Grün, M.; Schüth, F.; Unger, K. K. Pore Size Analysis of MCM-41 Type Adsorbents by Means of Nitrogen and Argon Adsorption. *J. Colloid Interface Sci.* **1998**, *207*, 159−169.
(46) Iler, R. K. *The Chemistry of Silica: Solubility, Polymerization, Colloid and Surface Properties, and Biochemistry of Silica*; Wiley: New York, 1979; p 897.
(47) Wu, S.-H.; Wu, C.-Y.; Lin, H.-P. Synthesis of Mesoporous Silica Nanoparticles. *Chem. Soc. Rev.* **2013**, *42*, 3862.
(48) Shchukin, D. G.; Shchukina, E. Capsules with External Navigation and Triggered Release. *Curr. Opin. Pharmacol.* **2014**, *18*, 42−46.
(49) Zheng, Z.; Huang, X.; Schenderlein, M.; Borisova, D.; Cao, R.; Möhwald, H.; Shchukin, D. Self-Healing and Antifouling Multifunctional Coatings Based on pH and Sulfide Ion Sensitive Nanocontainers. *Adv. Funct. Mater.* **2013**, *23*, 3307−3314.
(50) Kügler, R.; Bouloussa, O.; Rondelez, F. Evidence of a Charge-Density Threshold for Optimum Efficiency of Biocidal Cationic Surfaces. *Microbiology* **2005**, *151*, 1341−1348.
(51) Chen, C. Z.; Beck-Tan, N. C.; Dhurjati, P.; van Dyk, T. K.; LaRossa, R. A.; Cooper, S. L. Quaternary Ammonium Functionalized Poly(propylene Imine) Dendrimers as Effective Antimicrobials: Structure-Activity Studies. *Biomacromolecules* **2000**, *1*, 473−480.
(52) Majumdar, P.; Lee, E.; Gubbins, N.; Christianson, D. A.; Stafslien, S. J.; Daniels, J.; VanderWal, L.; Bahr, J.; Chisholm, B. J. Combinatorial Materials Research Applied to the Development of New Surface Coatings XIII: An Investigation of Polysiloxane Antimicrobial Coatings Containing Tethered Quaternary Ammonium Salt Groups. *J. Comb. Chem.* **2009**, *11*, 1115−1127.
(53) Schneider, C. A.; Rasband, W. S.; Eliceiri, K. W. NIH Image to ImageJ: 25 Years of Image Analysis. *Nat. Methods* **2012**, *9*, 671−675.

DOI: 10.1021/acsami.7b14642
ACS Appl. Mater. Interfaces 2017, 9, 38364−38372